Available online at www.sciencedirect.com
SCIENCE DIRECT®
International Journal of Heat and Mass Transfer 49 (2006) 2044–2052
International Journal of HEAT and MASS TRANSFER
www.elsevier.com/locate/ijhmt

Oscillatory nucleation in counter flows of vapor and droplets

S.P. Fisenko [a,*], M. Rusyniak [b], D.B. Kane [b], M.S. El-Shall [b]

[a] A.V. Luikov Heat and Mass Transfer Institute, National Academy of Sciences, 15 P. Brovka Street, Minsk 220072, Belarus
[b] Department of Chemistry, Virginia Commonwealth University, 1001 W. Main Street, Richmond, VA 23284, USA

Received 16 September 2005
Available online 20 March 2006

Abstract

Oscillatory nucleation regime in counter flows of vapor and falling droplets is considered. Experiments with such system were made in a diffusion cloud chamber. Oscillation is the results of the feedback between vapor depletion due to condensation on droplets and the value of a supersaturation in nucleation zone. For different pressure of carrier gas (helium) and temperatures, experimental results are presented for dodecane vapor. The new mathematical model of oscillatory nucleation is developed. Three characteristic times defines the duration of the process: nucleation time, time of droplets growth and falling, and, time of diffusion restoration of vapor profile. Experimental data and calculate ones are in good agreement.

1. Introduction

Counter flows of a vapor–carrier gas mixture and droplets often can be found in many contact heat and mass transfer exchangers, chemical reactors and other devices. For example, such processes take place during evaporative cooling of falling water droplets in the counter flow of fresh air in cooling towers [1]. Experimental and theoretical investigation of the kinetics of phase transition in such highly nonuniform and nonequilibrium system face great difficulties, especially if feedback between the processes of heat and mass transfer and phase transition are considered. This manifestation, which can be a release of the latent heat of a phase transition or a depletion of vapor composition, leads to strongly nonlinear processes in the systems. One such process is an oscillatory nucleation. We start the investigation of oscillatory nucleation in counter flows, first by considering this phenomena in a diffusion cloud chamber (DCC), where the relevant parameters are well controlled during experiments, and the theoretical investigation of the one-dimensional processes has high accuracy. In the DCC, all processes may be accurately described by the one dimensional approximation.

The diffusion cloud chamber provides excellent opportunities for simulation of oscillatory nucleation in counter flows (see Fig. 1). The flow of falling and growing droplets is one flow; the diffusion vapor flow is the counter flow [2]. It is well known that the highly nonequilibrium but steady-state medium in the DCC is an amplifier of weak signals; in particular, it is a sensitive detector of some trace impurities in a vapor [3]. Nucleation is a channel for the relaxation of the nonequilibrium medium.

To create higher nonequilibrium states, the temperature difference between plates of the DCC has to be increased. At some point the nonlinear effects of mass transfer interaction between new phase particles and counter diffusion flow of vapor, result in the breakdown of the steady-state condition of chamber performance, and the system undergoes a transition from steady-state behavior to stable oscillatory behavior with one basic frequency. The phenomenon of oscillatory nucleation in counter flows in the DCC was described in Ref. [4]. It is worth to note that oscillatory nucleation is a beautiful picture during visualization experiments.

According to the Le Chatelier's principle [5], this transition from steady-state mode to the oscillatory mode is a

* Corresponding author.
E-mail address: fsp@hmti.ac.by (S.P. Fisenko).

0017-9310/$ - see front matter © 2006 Elsevier Ltd. All rights reserved.
doi:10.1016/j.ijheatmasstransfer.2006.01.003

Nomenclature

A_i	amplitude of ith mode, m^{-3}
B	parameter, K
C	parameter, $m^3\ s^{-1}$
D	vapor diffusion coefficient, m^2/s
d	width of droplet cloud, m
T	temperature, K
g	the gravity acceleration, $m\ s^{-2}$
g^*	the number of molecules in the critical cluster, dimensionless
H	the chamber height, m
I	sink in diffusion equation, $m^{-3}\ s^{-1}$
J	nucleation rate, $m^{-3}\ s^{-1}$
k	Boltzmann's constant, $J\ K^{-1}$
L	mass transfer interpolation function, $m^4\ s^{-1}$
m	vapor molecule mass, kg
N	the number droplet per unit of volume in the cloud, m^{-3}
n	the number density of vapor, m^{-3}
P	pressure, Pa
R	droplet radius, m
S	supersaturation, dimensionless
t	time, s
t^*	restoration time of the first mode, s
t_s	temporal width of droplet cloud, s
v	velocity of droplet cloud, m/s
x	spatial variable, m
z	droplet position, m
z_s	saddle point height, m

Greek symbols

λ_v	the mean free path of vapor molecule
ρ_l	liquid density, $kg\ m^{-3}$
τ_l	nucleation time, s

Subscripts

0	initial
b	bottom plate
i	the number of modes
l	the linear profile
s	saddle point of free energy of cluster formation
sat	saturated
u	upper plate

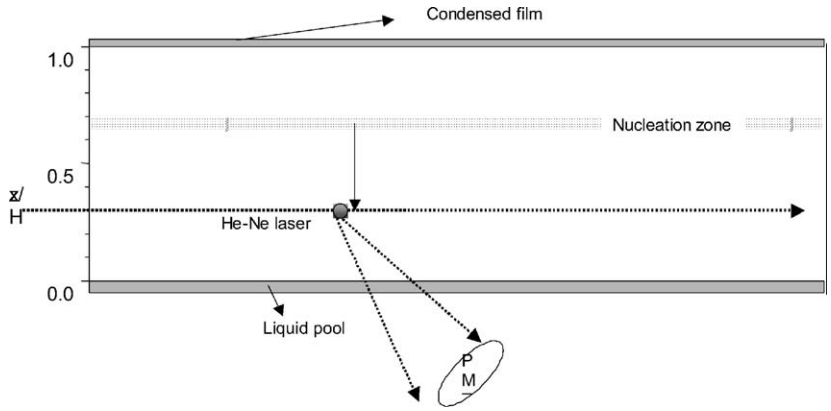

Fig. 1. The relative positions of the nucleation zone and detecting He–Ne laser in a diffusion cloud chamber.

reaction of a thermodynamic system after it was pushed to more nonequilibrium state. In particular, in the case being considered this transition is to decrease the supersaturation value in nucleation zone, as a supersaturation is the measure of a metastability of the system.

The physical mechanism of the oscillatory nucleation in DCC is the following. Droplets start to grow in the nucleation zone of a DCC. The growth of new phase particle leads to vapor depletion in this zone and in the upper part of the chamber. The larger the number density of droplets the larger vapor depletion due to the condensation process. Relatively large droplets begin to fall with increasing velocity, as the gravity is proportional to the cube of the droplet radius and the drag force is proportional only to the droplet radius in the approximation of a continuous medium. The contribution of thermophoresis is important only for droplets of nanometer scale. The vapor condensation on falling droplets leads to further vapor depletion. The nucleation rate, which affects on the number density of droplets, is very sensitive to vapor density. When the vapor flow into the nucleation zone is depleted nucleation practically stops, which decreases the vapor depletions. Finally, after the drops fall to the liquid pool at the bottom of the chamber, the diffusion restores the vapor profile and nucleation starts again. The aim of this work is to give a theoretical description, (which does not use empirical parameters), for the interconnected heat and mass transfer processes affecting on the basic parameters of the oscillatory nucleation in DCC.

The problems of describing a feedback mechanism, related to condensation in aerosol systems, were discussed

earlier in an important work [6]. General consideration of the conditions giving rise to oscillation in a nonlinear system with feedback is given in [7].

The outlook of paper is the following. We present our experimental data in chapter two. The new nonlinear mathematical model of oscillatory nucleation is described in the third chapter. Finally, we discuss and summarize our results.

Preliminary results of this investigation have been published in [8].

2. Description of experiments

Detailed descriptions of the design and use of DCC have been given elsewhere [2, and the references therein], so only a brief description of the experimental setup, and experiments performed in the oscillatory regime is given here. The schematic drawing of the DCC is shown in Fig. 1. The DCC consists of a cooled top and heated bottom plate separated by a glass ring. The surfaces of both plates are coated with a thin film of the nucleating fluid. The temperatures of the top and bottom plates are controlled by circulating fluids from temperature controlled reservoirs (not shown in the drawing). In operation the sample liquid evaporates from the warm bottom plate, and vapor diffuses upward through a carrier gas to condense on the cooler upper plate. The geometry of the chamber is such that the temperature and supersaturation profiles within the chamber can be accurately calculated by solving the one-dimensional heat and mass transfer problem. The measured chamber parameters, total pressure, temperature at the surface of the liquid pool, and temperature of the upper plate provide the necessary boundary conditions for the calculation. When the supersaturation is large enough homogeneous nucleation of the vapor occurs in a zone of finite width, approximately 10% of the total chamber height (H), around the plane in which the maximum nucleation rate occurs ($\sim 0.7H$). Due to the small size ($\sim$1 nm) and transient nature of the condensation nucleus it cannot be directly detected. It is only after the nucleus has grown several orders of magnitude to around 25 μm the result of nucleation is detected. In the experiments described here nucleation is detected the forward scattering light from a helium–neon laser by the macroscopic droplets falling from the nucleation zone. A photomultiplier was used to collect the scattered light signal. The output of the photomultiplier was digitized using an analog to digital converter on a computer and a fast Fourier transformation (FFT) of the signal gave the oscillation frequency.

For these experiments the chamber height $H = 5$ cm and the temperature difference between the bottom and top surfaces was approximately 120 K. The dodecane used as the nucleating fluid was obtained from Aldrich with stated purity of at least 99% and was degassed repeatedly by the freeze–pump–thaw method and transferred to the cloud chamber under vacuum. The carrier gas was research grade helium (99.999% pure). The thermophysical properties of dodecane are given in Ref. [2]. The dependence of the frequency of oscillations on both temperature and pressure was investigated.

In the regime of the oscillatory nucleation, droplets are formed in discreet clouds or pulses. The signal from the photomultiplier displayed in Fig. 2 shows the distinct periodic nature of this regime. The chamber parameters for the measurements in Fig. 2 are given in Table 1. In Fig. 2 it is observed that as the temperature difference between the top and bottom surfaces increases the scattered light signal transitions from random to weak and then to strong oscillations. It is important to emphasize that these experiments were conducted in such manner that the temperature was approximately constant at position of the maximum nucleation rate for all the experiments.

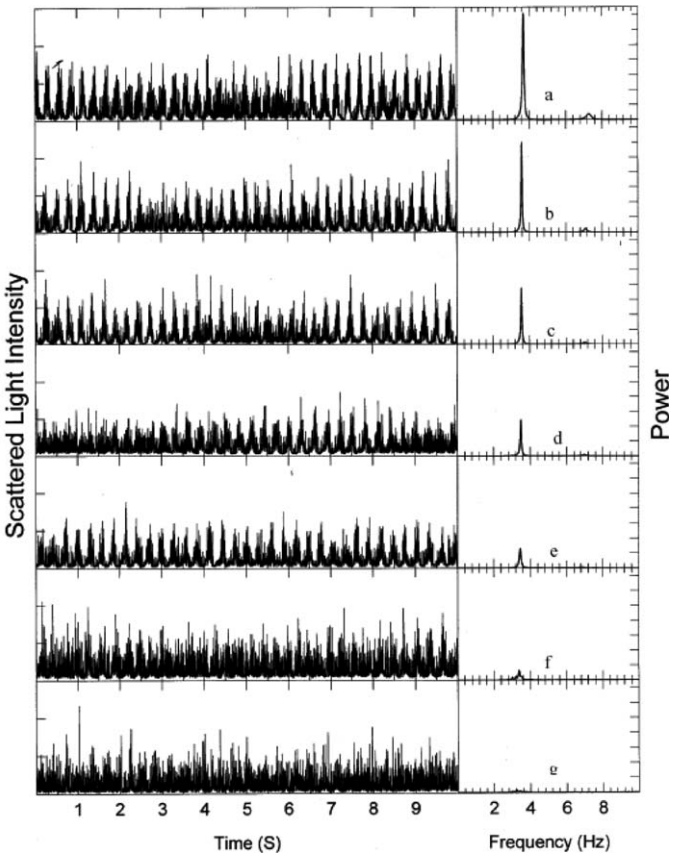

Fig. 2. The scattered light signal caused by nucleated particles in the diffusion cloud chamber and corresponding power spectrum.

Table 1

Experiments	T_b	T_u	P (Pa)
a	396.62	278.18	1.18×10^4
b	393.32	278.05	1.137×10^4
c	392.28	278.15	1.13×10^4
d	390.92	277.85	1.11×10^4
e	389.02	277.92	1.093×10^4
f	377.5	278.6	1.03×10^4
g	365.65	279.52	9.4×10^3

A strong correlation is apparent between the temperature difference ($T_b - T_u$) and intensity of scattering light by droplet cloud, presented in Fig. 2, while there is only a weak correlation between the temperature difference and the period of oscillation. This implies that the temperature difference affects both the nucleation process and the droplet growth process, and the feedback mechanism that causes oscillatory nucleation compensates for increases in the temperature difference. As many of the parameters within DCC cannot be directly measured mathematical simulation of oscillatory nucleation behavior can provide significant insight of the performance of this feedback mechanism.

3. Mathematical model

The aim of the mathematical model is to calculate the basic parameters of oscillatory nucleation in DCC, do not using empirical fitting parameters. In fact, we will simulate the process shown in Fig. 3, which is the idealization of the experimental results. Simulation of the interrelation between of shape of optical signal and nucleation process in DCC would require a more powerful mathematical model.

The number density of the vapor molecules, $n(x,t)$, is governed by the diffusion equation with moving sink of variable intensity (the cloud of falling and growing droplets)

$$\partial_t n(x,t) = \partial_x[D(T(x))\partial_x n(x,t)] - I(R(z(t)), \langle n(z(t),t)\rangle), \quad (1)$$

where $\langle n(z(t),t)\rangle$ is the average vapor density near the center of mass of the droplet cloud, $D(T(x))$ is the temperature dependent diffusion coefficient, $T(x)$ is the temperature profile, I is a function that describes the condensation of vapor on the moving droplets, $R(z(t))$ and $z(t)$ are the average radius and position of droplet in the cloud respectively.

The position of droplet cloud, $z(t)$, is determined by the equation

$$\frac{dz}{dt} = v(R, \langle n(z(t),t)\rangle), \quad (2)$$

v is the velocity of the droplet cloud, is determined by the drag, gravitational, and thermophoretic forces on the droplets in the cloud. Since a steady-state velocity is reached in less than 10^{-7} s [9], the velocity the droplets of a given radius can be determined from the equilibrium of these forces.

Droplet growth is described by the following equation:

$$\frac{dR(t)}{dt} = L(R)[\langle n(z(t),t)\rangle - \langle n_{sat}(z(t))\rangle], \quad (3)$$

where $n_{sat}(z(t))$ is the number density of saturated vapor for corresponding temperature, L describes isothermal mass transfer between droplet and vapor and is a nonlinear function of the Knudsen number [9]. Exact expressions for the function L are available for both the free molecular and the diffusion regimes, and in the transition regimes the interpolation is used [9].

The expression for the vapor sink I is

$$I = 4\pi R^2 N L(R)[\langle n(z(t),t)\rangle - \langle n_{sat}[T(z(t))]\rangle]\rho_l/m, \quad (4)$$

where N is the number density of droplets in the cloud, the ρ_l and m, are, correspondingly, mass density and the mass per molecule of the condensing material.

To combine analytical and numerical analysis of oscillatory phenomena, we use the Galerkin method below [7]. Then the number density of a vapor is given by

$$n(x,t) = n_l(x) + \sum_i A_i(t)\sin\left(\frac{\pi x i}{H}\right), \quad (5)$$

where sine functions are chosen as trial functions, $A_i(t)$ are unknown amplitudes of these modes (trial functions). The linear vapor profile $n_l(x)$ exactly satisfies to the boundary conditions:

$$n_l(x) = n_b + \frac{(n_u - n_b)x}{H}, \quad (6)$$

where n_b and n_u, are, correspondingly, saturated vapor density, for temperatures T_b and T_u at the top and bottom of the DCC.

The averaged vapor density in the droplet cloud $\langle n(z(t),t)\rangle$ is determined from

$$\langle n(z(t),t)\rangle = \frac{1}{d}\int_{z-0.5d}^{z+0.5d} n(y,t)\,dy, \quad (7)$$

where d is the width of droplet cloud in the steady-state regime [9,11]. Similarly, the averaged value of saturated vapor in the cloud $\langle n_{sat}(z)\rangle$, is determined by the expression:

$$\langle n_{sat}(z)\rangle = \frac{1}{d}\int_{z-0.5d}^{z+0.5d} n_{sat}[T(y)]\,dy.$$

Since the partial pressure of helium is much larger than partial pressure of dodecane for all the experiments presented here, it is reasonable to assume that the heat conductivity removes the latent heat of the phase transition in DCC. Therefore, the steady-state solution to the temperature profile in the DCC can be used in simulating oscillatory nucleation. If the heat transfer played a substantial roll in the oscillatory nucleation process, two independent oscillation frequencies would be expected in the experimen-

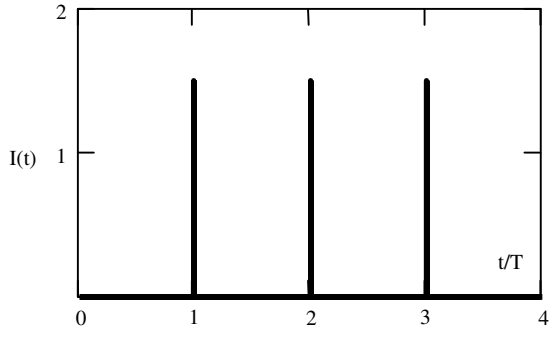

Fig. 3. The idealized oscillatory process to be simulated by the mathematical model. T is the period of oscillation.

tal data. Since the of Fourier transformation of experimental data shown in Fig. 2 indicates that there is only one independent fundamental frequency, there is experimental confirmation that the steady-state temperature profile is maintained within the DCC during oscillatory nucleation. In DCC the steady-state temperature profile $T(x)$ is given by the expression:

$$T(x) = T_b + (T_u - T_b)x/H + B\sin(\pi x/H), \tag{8}$$

where T_b is the temperature of the surface liquid pool on the bottom of the chamber, T_u is the temperature of liquid film on the top plate of the chamber. An iterative procedure to calculate the parameter B is described in Ref. [11]. Expression (8) takes into account two important factors: concentration and the temperature dependence of the thermal conductivity coefficient of a helium–vapor mixture [12]. The steady-state temperature profile is shown in Fig. 4. As the concentration of helium increases near top plate of DCC, it increases the effective heat conductivity of the helium–dodecane mixture. To conserve the heat flow through the chamber, the temperature gradient has to decrease, therefore in the expression (8) the parameter $B < 0$. This effect is clearly seen in Fig. 4. In contrast, the diffusion coefficient decreases with the decreasing temperature near top surface of the cloud chamber, so the vapor gradient increases in comparison with gradient near bottom surface. For experimental runs displayed in Fig. 2, our simulation, based on the new mathematical model, shows that the temperature of the vapor–carrier gas mixture at the saddle point of the free energy of formation surface, T_s, is 297 K for all the experiments and the saddle point is at the same height for all experiments.

Substituting Eq. (5) into Eq. (1), after standard transformations related to the Galerkin method, a system of ordinary differential equations for amplitudes A_i is obtained [10]. In particular, for the amplitude of the first mode A_1 we have the following equation:

$$\frac{dA_1(t)}{dt} = -\frac{2\pi}{H^3}(n_u - n_b)C_1 - \frac{2\pi^2}{H^3}\sum_{i=1} iA_iC_{1i} - \frac{16R^2NL[R(z,t)]\rho_1}{m}\left[n_l(z) - \langle n_{sat}(z(t))\rangle - \frac{2H}{d\pi}\sum_i \frac{A_i}{i}\sin(i\pi z/H)\sin(id\pi/2H)\right] \tag{9}$$

and

$$C_1 = \int_0^H D(T(x))\cos(\pi x/H)\,dx.$$

The integral, arising from the calculation of the first mode, is equal

$$\int_0^H \sin^2(\pi x/H)\,dx = H/2.$$

Actually C_1 determines the averaged vapor diffusion coefficient for temperature profile (8). The terms C_{1i} take into account the diffusion interaction between the first mode and ith mode of the number density of the vapor. This interaction between the modes arises because vapor diffusion coefficient strongly depends on a temperature of a mixture and due to vapor condensation on droplets. C_{1i} is expressed

$$C_{1i} = \int_0^H D(T(x))\cos(\pi x/H)\cos(i\pi x/H)\,dx.$$

The equations for A_i have a similar form.

The more modes used in the calculation the more precise the description of the mass transfer processes in DCC. In the results below the first seven modes are used, because the characteristic spatial dimension of the seventh mode is already approximately equal to the width of nucleation zone. The numerical results of the model show that seven modes are enough for an accurate description of the oscillations vapor density in DCC.

For the system of Eqs. (1)–(3) boundary conditions are

$$n(0,t) = n_{sat}(T_b) = n_b, \tag{10}$$

$$n(H,t) = n_{sat}(T_u) = n_u. \tag{11}$$

The initial position of the droplet cloud $z(0)$ coincides with the position of the saddle point, z_s, of the free energy of cluster formation surface [9], we have

$$z(0) = z_s, \tag{12}$$

$$A_i(0) = A0_i, \tag{13}$$

where $A0_i$ are arbitrary constants depending on the initial vapor profile.

The system of ODE with the boundary conditions (10)–(13) can be used for many purposes. If it is assumed that $N = 0$, an analytical form the steady-state vapor profile in the DCC can be obtained. Using this steady-state vapor

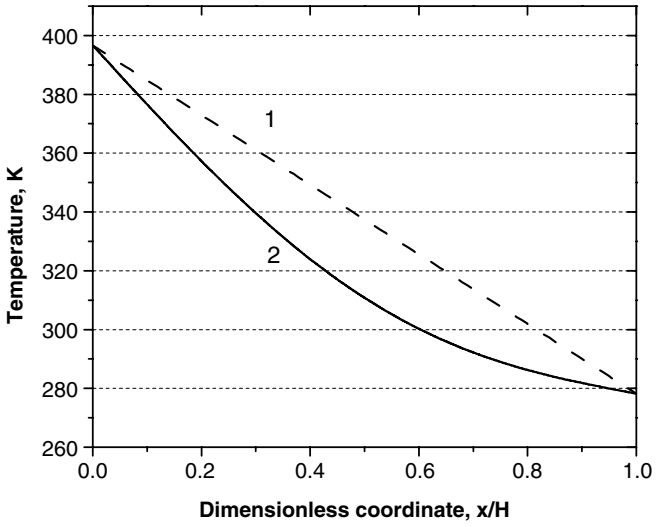

Fig. 4. The steady-state temperature profile for the gas–vapor mixture in the diffusion cloud chamber for the conditions of run a. ($T_u = 278$ K, $T_b = 397$ K, $P_{tot} = 1.2 \times 10^4$). Curve 1 is calculated with a linear approximation of the profile and curve 2 is a steady-state solution obtained by Galerkin's method.

profile the value of vapor molecule number density at the saddle point of free energy cluster formation surface, n_s, can be determined. To obtain the dimensionless value of the amplitudes A_i as shown in Figs. 6 and 7, we use n_s as the scale. Only the first two amplitudes significantly affect the vapor profiles in the chamber during oscillation. Therefore, initially the steady-state values of all seven amplitudes are calculated and used as initial amplitudes for the third and higher modes during the simulation of the oscillatory nucleation.

To illustrate for run (a) in Fig. 2: $z_s/H = 0.65$, $n_b = 1 \times 10^{24}$ mol/m^3, $n_u = 7.8 \times 10^{20}$ mol/m^3, and $n_s = 3.6 \times 10^{23}$ mol/m^3. Assuming a linear vapor profile at z_s would give $n_l(z_s) = 3.5 \times 10^{23}$ mol/m^3. Calculation shows that for the dodecane–helium mixture the steady-state vapor profile is convex compared to the temperature profile.

4. Simulation of oscillatory regime nucleation

For conditions experiment 'a' the position of the droplet cloud during a single period of oscillation is displayed in Fig. 5a; the averaged droplet radius in the cloud versus time is shown in Fig. 5b. As seen in Fig. 5a there is a substantial period (about 0.01 s) during which the droplets do not move from nucleation zone, because the gravity is practically get balanced by thermophoretic force. In addition, the height where the droplet radius reaches 25 μm is close to the position of the saddle point on free energy surface [9]. Thus, our simulations confirm that the height at which the droplets become visible is the same for all experiments presented in Fig. 2. As seen in Fig. 5 larger droplets have a larger velocity, therefore under conditions of diffusion-controlled growth, larger droplets have smaller impact on vapor profile (also see Fig. 8).

It is obvious that N is an important parameter in our mathematical model. In principle, it can be measured experimentally, but with our experimental setup it was not practical to make this measurement. Therefore the mathematical mode for oscillatory regime of homogeneous nucleation in a DCC has three adjustable parameters: N and the amplitudes of the first two modes: A_1 and A_2. We have to use only one experimental result, the oscillation period. Due to the rapid relaxation of the amplitudes of other modes, we assume that initially all of the high mode amplitudes are equal to their steady-state values.

A procedure has been developed to determine the values of these three parameters using the available experimental data and classical nucleation theory. There is only a limited range of droplet concentrations, N, which will produce oscillations of a given period. The first step is to determine the value of N that produces oscillations close to the experimentally determined frequency. Once this value has been determined the amplitudes of the first two modes at the start of nucleation are determined by an iterative process by trying to minimize the difference between the experimentally measured and calculated periods of oscillation. Using

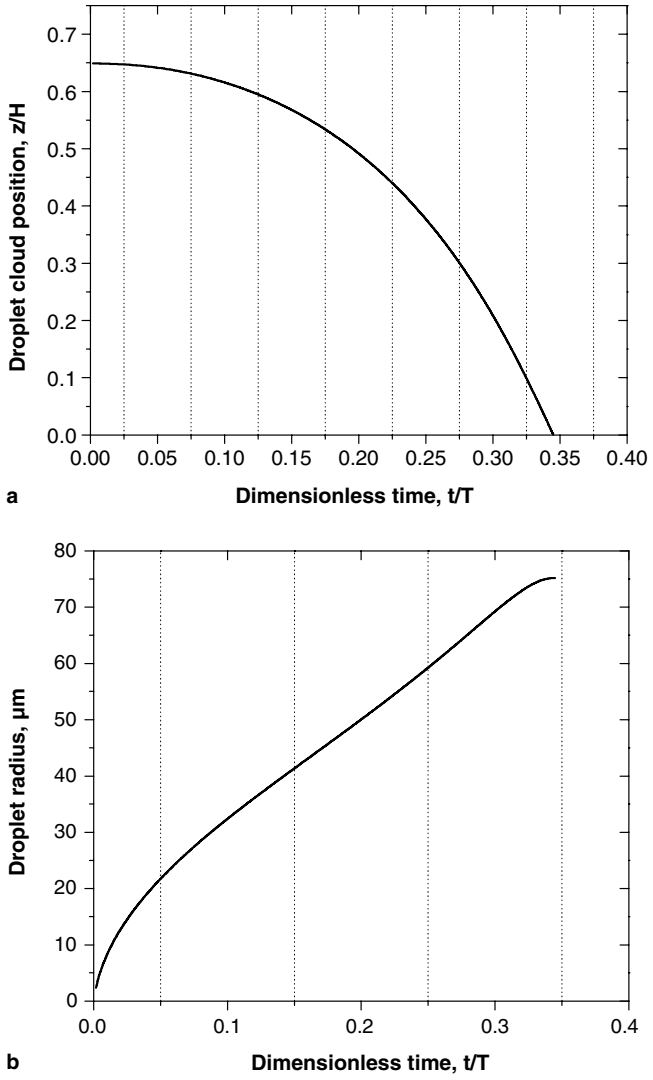

Fig. 5. The dimensionless position of droplet cloud (a) and droplet radius (b) in microns over a period of oscillation for the conditions of run (a).

these amplitudes as the initial values for the system of Eqs. (1)–(3) we can now solve of our mathematical model numerically. The model results must be self-consistent with classical nucleation theory. This condition means that for given N, the fraction N/J has to have the same order of the as τ_1, where τ_1 time interval during which the amplitude of the first mode is constant (the time over which nucleation occurs during an oscillation); J is the classical nucleation rate calculated from the supersaturation and temperature at the saddle point of the free energy of formation surface in DCC. The value of N for the calculated supersaturation can be determined with logarithmic accuracy, accuracy comparable to the accuracy of modern cloud chamber measurements. The value of τ_1 determined directly from simulation. Thus, the oscillation period and the self-consistency condition help to determine all three unknown parameters of mathematical model.

In particular, it was found that for run a, $N = 5 \times 10^5$ droplets/m^3. This means also that the average distance

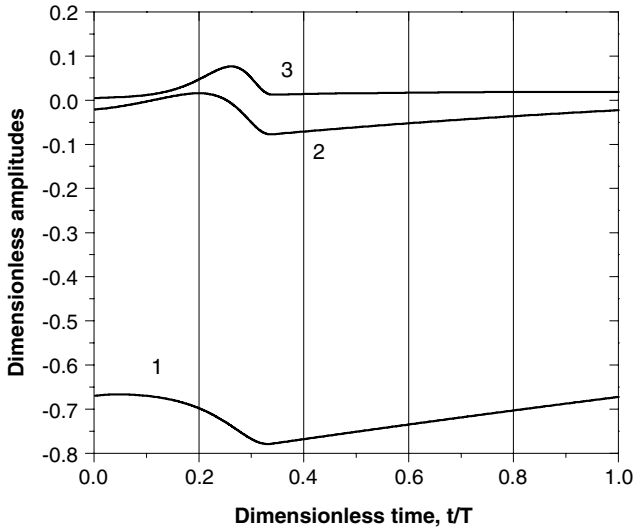

Fig. 6. The evolution of dimensionless amplitudes of the first three modes ($i = 1,2,3$) over a single period (T) for the conditions of run (a). Curve 1 is the first mode, curve 2 is the second mode, curve 3 is the third mode.

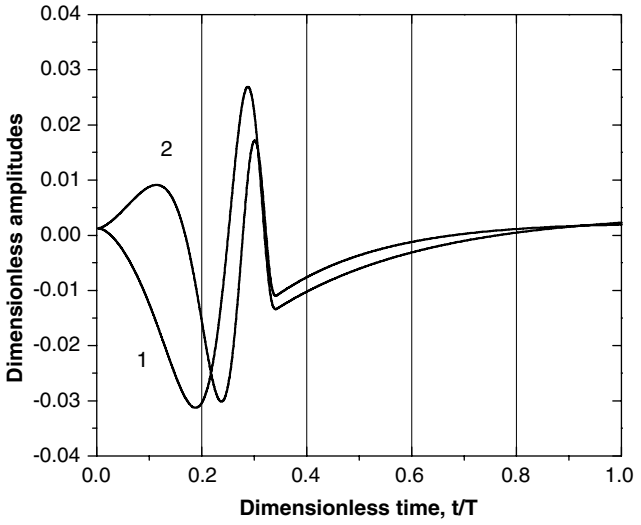

Fig. 7. The evolution of the dimensionless amplitudes of fourth and fifth modes over a single period (T) for the conditions of run (a). Curve 1 is the fourth mode, curve 2 is the fifth mode.

between droplets in the cloud is much larger their radii and we can consider their growth independently each other.

The evolutions of amplitudes of first three modes for a oscillation period are shown in Fig. 6. The change of amplitude of the first mode is large in comparison with the amplitudes of higher modes. This computational fact emphasizes the importance of accurately describing the first mode for modeling oscillatory nucleation. The relaxation time of the third mode is very short compared with the first two. The excitation of the third mode is due to interactions between the modes in the nonlinear model and the vapor condensation on the droplets. The simulations show that only the interactions between neighboring modes are of substantial importance. As the number of the mode increases the maximum amplitude of the mode decreases, and it takes less time to reach the steady-state value after droplet cloud reaches the bottom of the chamber. The evolution of the amplitudes A_4 and A_5 is shown in Fig. 7. The steady-state values of the amplitudes are not equal to zero, however the time required to restore these steady-state value is shorter that for the first mode. The characteristic times of relaxation of ith mode decreases according to the law i^{-2}. The range of amplitudes of the higher order modes is much smaller; therefore it is their contributions to the vapor density is insignificant. For the chamber conditions of the experiments presented in Fig. 2 the maximum amplitude of the higher modes ($i > 3$) is practically the same, although shapes of curves differ slightly. The smaller the temperature difference across the chamber, the smaller the rate of change of all the amplitudes.

The supersaturation profile $S(x,t)$ is calculated from

$$S(x,t) = n(x,t)/n_{\mathrm{sat}}[T(x)],$$

where n_{sat} is the number density of the saturated vapor at the temperature $T(x)$. For the conditions of run (a) the supersaturation profiles are shown in Fig. 8 at different instances during the oscillation.

Near the bottom ($x < 0.3H$) and the top ($x > 0.85H$) of the chamber the supersaturation remains practically constant throughout the oscillation. In the lower part of the chamber the velocity of the falling droplets is high, so their residence time is small enough that the cloud has only a minimal effect on the vapor density. The supersaturation near the saddle point ($z_s \sim 0.65H$) changes significantly, during and after nucleation. The instantaneous nucleation rate decreases by several orders of magnitude when the supersaturation has dropped about 6%. The effects of droplet growth and motion expand the spatial disturbances of the supersaturation profile. After the droplet cloud falls to

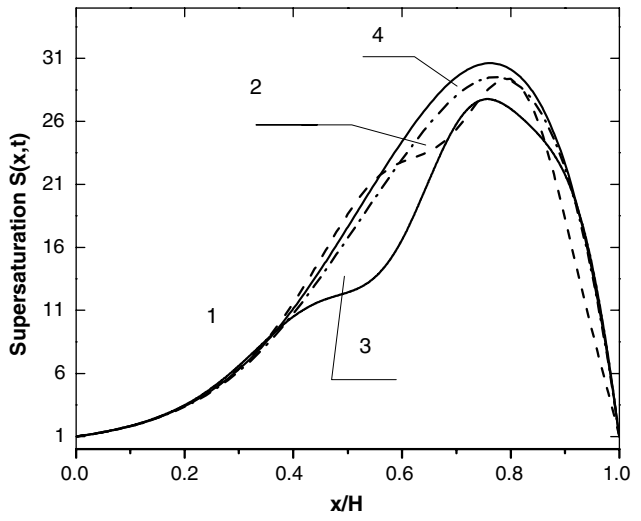

Fig. 8. Supersaturation profiles in the diffusion cloud chamber at different moments within a period of oscillation. Curve 1 is at the beginning of nucleation ($t = 0$ s), curve 2 is at $t = 0.024$ s (just after nucleation stops); curve 3 is at $t = 0.07$ s, curve 4 is at $t = 0.245$ s while the diffusion process restores the vapor profile. The period of is 0.296 s.

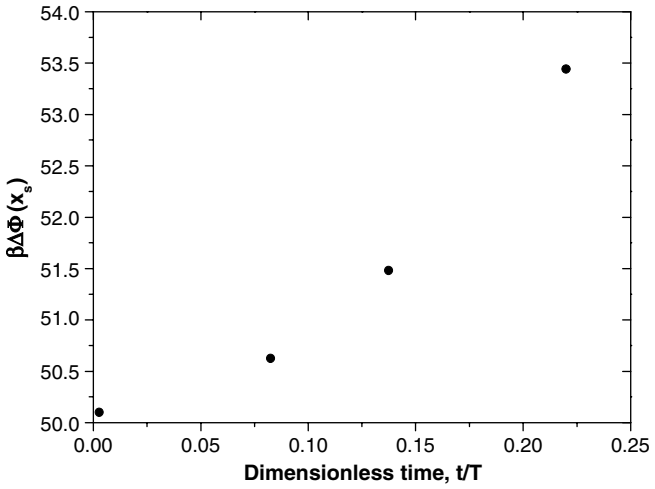

Fig. 9. The dimensionless free energy of formation of the critical cluster ($\Delta\Phi\beta$) at the position of the maximum nucleation rate plane in the diffusion cloud chamber at various times during an oscillation.

the bottom, the restoration process is fastest in the upper part of chamber because of the relatively low vapor density.

The dimensionless free energy formation for the critical cluster formation at the saddle point height z_s is shown as a function of time in Fig. 9. We see that during a short period of time, which is about ten percentage of the oscillation period the dimensionless free energy increases due to the vapor depletion. This corresponds to a drop in the nucleation rate of more than two orders of the magnitude.

It follows from our results that there are three characteristic times for oscillatory nucleation: a relatively short nucleation time, significantly longer time for the droplets growth and fall, and a relaxation time. The relaxation time is even longer time (about 2/3 of oscillation period) for diffusion to restore the vapor profile.

5. Results and discussion

We did the experimental investigation of oscillatory regime of diffusion cloud chamber (DCC) for mixture of helium and dodecane vapor. The experiments were organized in such matter that for all experiments the temperature at the plane of maximum nucleation rate were practically the same. The digitalized data of intensity of scattering light on falling droplets has been obtained. From the scattered light signal of the falling droplets we discovered that there is only one the basic frequency of the oscillatory nucleation. Although the total pressure has a significant effect on the droplet growth rate in nucleation experiments [9], the fundamental frequency of the oscillations in the DCC did not exhibit a significant dependence on the total pressure of the vapor gas mixture in the chamber. The both time to deplete and the time to restore of the vapor concentration around the nucleation zone are directly proportional to the diffusion coefficient. Moreover, it was found that the visualization position of droplet cloud is practically the same for all experimental conditions in the table.

Analysis shown that the single basic frequency means that the heat processes has a steady-state character in DCC. For avoiding the free convection in DCC the partial pressure of the carrier gas (helium) must be significantly higher than the partial pressure of the vapor. Therefore, the heat transfer processes are practically not affected by the changes in the vapor concentration near the nucleation zone and maintain the steady-state character. This is if different from the vast majority instances with oscillatory phase transition phenomena where the release of the latent heat of the phase transition plays main role.

New nonlinear mathematical model of oscillatory nucleation in a DCC is developed. This model includes the feedback between nucleation rate from one side and heat and mass transfer in gaseous phase and droplets growth and motion, from another side. Simulations, based on new mathematical model, shown that the period of oscillation is equal to sum of the durations of two processes: time of droplet falling on the bottom chamber and the diffusion restoration time. Diffusion restoration time is the time of restoration of vapor profile in the nucleation zone after falling of droplet cloud on the bottom of the chamber. The shape of intensity of scattering light, shown in Fig. 2, is the results of a finite width of nucleation zone.

It is worth to make the estimation of the oscillation period in diffusion cloud chamber. For typical DCC the width of nucleation zone d is about $0.1H$ and it is situated at the height z_s is about $0.6–0.7H$ [9]. Then the estimation of the falling time t_f is

$$t_f \sim \sqrt{\frac{2z_s}{g}}, \tag{14}$$

where g is the gravity. For our DCC, we have that $t_f \sim 0.085$ s, that well corresponds with numerical results for run a.

An estimation of the restoration time for the first mode, t^*, can be obtained using the Galerkin method [10,13]. The approximate formula for t^* is

$$t^* = -\frac{H^2}{D\pi^2}\ln(0.1), \tag{15}$$

where D is the vapor diffusion coefficient . In particular, for conditions of our experiments we have from (15) $t^* \sim 0.12$ s. So, the sum of t_f and t^* is about 0.2 s, that agree reasonably well with experimental data.

From the simulation results it is apparent that the oscillatory nucleation takes place only if there is significant depletion of vapor in the nucleation zone of DCC. This will occur when the droplet diameter becomes larger than the mean free path of the vapor molecules, λ_v [9], because vapor condensation on droplets is most substantial when droplets are large enough. In other words, when the Knudsen number, defined as $Kn = \lambda_v/R$, less than 0.1. From the simulation data and comparing terms at the Eq. (1), it can be established that oscillatory nucleation takes place if the dimensionless parameter $C > 0.05$, where

$$C = 4\pi N(10\lambda_v)H^2. \quad (16)$$

The parameter C is an estimate of the relationship between the two terms on the right-hand side of Eq. (1). If number and size of droplets are large enough and $C > 0.05$, the droplet cloud will create a significant depletion of the vapor concentration in nucleation zone. C has a strong dependence on the chamber height, H, which results from that the role that the diffusion mechanism for transporting the vapor plays in the oscillatory nucleation. This is a substantial deviation from the simplified mathematical model of oscillatory nucleation in DCC developed by Brito and Heist [4]. When C is $\leqslant 0.05$, small amplitude oscillations of nucleation rate are observed as shown in Fig. 2g. For substances with similar diffusion coefficients and nucleation zone parameters it is expected that the fundamental frequency will be nearly equal, but the amplitude of the vapor oscillation depends on the product $N(10\lambda_v)$ and may vary significantly.

The value of N at which a vapor depletion effect large enough to stop the nucleation process can be obtained from [6]

$$J(n) = J(n_0)\left(\frac{n}{n_0}\right)^{g^*+2}, \quad (17)$$

where g^* is the number of molecule at a critical cluster. The equation describes the change in the nucleation rate if the number density of vapor changes from n_0 to n. For $g^* \sim 30$ (a typical value for the critical cluster size of dodecane in the nucleation zone for the experiments presented here) a 5% depletion of the vapor density would decrease the nucleation rate by more than one order of magnitude. The model shows that that the vapor density decreases by 6–7% of its maximum value during the oscillations observed in Fig. 2.

Using the model additional information about the droplet cloud can be extracted from the limited experimental data. In particular, we have that the effective nucleation rate J during the particle creation phase of an oscillation is equal to $J \approx 2 \times 10^7$ droplet/s m^3; the dimensionless free energy of formation for the critical cluster $\Delta\Phi/kT_s$, is equal to 50.2. For the steady-state regime of nucleation at the same T_s our calculation gives that $\Delta\Phi/kT_s \approx 57$. The difference is the number of created droplets per unit of volume in the cloud, N, and the duration of the nucleation period. The larger the diffusion driven flow the later depletion starts and, correspondingly the longer the duration of the nucleation period. The intensity of the diffusion flow is mainly determined by the temperature difference $T_b - T_u$ and vapor nature.

As the simulation demonstrates, the width of the scattered light peaks presented in Fig. 2 reflects the width of nucleation zone in DCC. Droplets formed in the lower part of the nucleation zone fall for a shorter time prior to reaching the He–Ne detection laser than droplets created near or above the saddle point of the cluster free energy surface in the chamber. A simple estimation based on expression (14) gives the characteristic temporal width t_s of the optical signal in Fig. 2

$$t_s \sim \sqrt{\frac{2z_s}{g}}\frac{d}{4z_s}$$

for experiment (a) t_s is about 6×10^{-3} s. Furthermore, the expression shows that the light pulse duration is practically the same for all the experimental results shown in Fig. 2, in agreement with what was observed experimentally.

The shape of signal gives data to investigate the problem of the finite width of the nucleation zone in cloud chamber. Currently, experimental methods cannot resolve nuclei created in different regions of the nucleation zone. Therefore valuable information about the spatial distribution of the nucleation rate is not available. In the framework of mathematical model developed here this information cannot be extract from experimental data. However a new, more powerful mathematical model is under development.

Finally to mention, that the experiments in DCC, at which impossible to neglect this diffusion interaction between growing droplets, are considered in [11].

References

[1] S.P. Fisenko, A.A. Brin, A.I. Petruchik, Evaporative cooling of water in a mechanical draft cooling tower, Int. J. Heat Mass Transfer 47 (2004) 165–177.
[2] M. Rusyniak, M.S. El-Shall, Vapor phase homogeneous nucleation of higher alkanes: dodecane, hexadecane and octadecane. 1. Critical supersaturation and nucleation rate measurements, J. Phys. Chem. B 105 (2001) 11866–11872.
[3] D. Kane, M.S. El-Shall, Ion nucleation as a detector: application of REMPI to generate selected ions in supersaturated vapors, Chem. Phys. Lett. 259 (1996) 482–487.
[4] J. Brito, R.H. Heist, Nucleation and growth in the diffusion cloud chamber. I. Oscillatory nucleation, Chem. Eng. Commun. 15 (1982) 133–149.
[5] E. Fermi, Thermodynamics, Dover, New York, 1956.
[6] R. McGraw, J. Saunders, A condensation feedback mechanism for oscillatory nucleation and growth, J. Aerosol. Sci. Technol. (1984) 367–380.
[7] D.V. Efimov, A.L. Fradkov, Oscillation conditions of nonlinear systems with static feedback, Automat. Rem. Control 66 (2005) 249–264.
[8] M. Rusyniak, S.P. Fisenko, M.S. El-Shall, Nucleation rate determination from measurements of oscillatory nucleation in diffusion cloud chamber, in: B. Hale, M. Kulmala (Eds.), Nucleation and Atmospheric Aerosols 2000, 15 Intern. Conference, vol. 534, American Institute of Physics Proceedings, 2000, pp. 171–174.
[9] D. Kane, S.P. Fisenko, M. Rusyniak, M.S. El-Shall, The effect of carrier gas pressure on vapor phase nucleation experiments using thermal diffusion cloud chamber, J. Chem. Phys. 111 (1999) 8496–8502.
[10] C.A.J. Fletcher, Computational Galerkin Methods, Springer-Verlag, New York, 1984.
[11] S.P. Fisenko, R.H. Heist, Puzzle of high-pressure nucleation experiments in diffusion cloud chambers, in: J. Schmelzer, G. Röpke, V. Priezzhev (Eds.), Nucleation Theory and its Applications, Dubna, Joint Institute of Nuclear Research Publishing Department, 2002, pp. 146–164.
[12] R.C. Reid, J.M. Prausnitz, B.E. Poling, The Properties of Gases & Liquids, McGraw-Hill, Boston, 1984.
[13] P. Morse, H. Fershbach, Methods of Theoretical Physics, McGraw-Hill, New York, 1999.